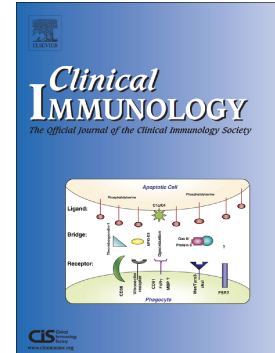


Th2 cell clonal expansion at diagnosis in human type 1 diabetes

Aditi Narsale, Francisco Almanza, Theo Tran, Breanna Lam, David Seo, Alisa Vu, S. Alice Long, Laura Cooney, Elisavet Serti, Joanna D. Davies



PII: S1521-6616(23)00592-2

DOI: <https://doi.org/10.1016/j.clim.2023.109829>

Reference: YCLIM 109829

To appear in: *Clinical Immunology*

Received date: 27 August 2023

Revised date: 26 October 2023

Accepted date: 27 October 2023

Please cite this article as: A. Narsale, F. Almanza, T. Tran, et al., Th2 cell clonal expansion at diagnosis in human type 1 diabetes, *Clinical Immunology* (2023), <https://doi.org/10.1016/j.clim.2023.109829>

This is a PDF file of an article that has undergone enhancements after acceptance, such as the addition of a cover page and metadata, and formatting for readability, but it is not yet the definitive version of record. This version will undergo additional copyediting, typesetting and review before it is published in its final form, but we are providing this version to give early visibility of the article. Please note that, during the production process, errors may be discovered which could affect the content, and all legal disclaimers that apply to the journal pertain.

Th2 cell clonal expansion at diagnosis in human type 1 diabetes

Aditi Narsale^a, Francisco Almanza^a, Theo Tran^a, Breanna Lam^{a1}, David Seo^a, Alisa Vu^a, S. Alice Long^b, Laura Cooney^c, Elisavet Serti^{d2}, Joanna D. Davies^{a,c}

^aSan Diego Biomedical Research Institute, 3525 John Hopkins Court, San Diego, California, 92121, U.S.A. anarsale@sdbri.org; falmanza@sdbri.org; theodore.m.tran@gmail.com; bhlam@mit.edu; vaidoubled@gmail.com; avu@sdbri.org

^bBenaroya Research Institute, 1201 9th Ave, Seattle, Washington, 98101, U.S.A. along@benaroyaresearch.org

^cImmune Tolerance Network, Ann Arbor, Michigan, U.S.A. lcooney@immunetolerance.org

^dImmune Tolerance Network, Bethesda, Maryland, U.S.A. ESertiChrisos@hivresearch.org

^eCorresponding author: Joanna D. Davies, San Diego Biomedical Research Institute, 3525 John Hopkins Court, San Diego, CA 92121, U.S.A. Tel: (858) 200-7048; Email: jdavies@sdbri.org

Present address

1. Massachusetts Institute of Technology, 77 Massachusetts Avenue, Cambridge, Massachusetts, 02139, U.S.A.

2. The Henry M. Jackson Foundation, 6720A Rockledge Drive, Suite 400, Bethesda, Maryland, 20817

Abbreviations list: LoR – Length of remission; ITN-Immune Tolerance Network; IDAA1c – Insulin dose adjusted A1c; IPA – Ingenuity Pathway Analysis; DGE – differential gene expression; Tfh – follicular helper T cells; HDM – house dust mite

Abstract

Soon after diagnosis with type 1 diabetes (T1D), many patients experience a period of partial remission. A longer partial remission is associated with a better response to treatment, but the mechanism is not known. The frequency of CD4⁺CD25⁺CD127^{hi} (127-hi) cells, a cell subset with an anti-inflammatory Th2 bias, correlates positively with length of partial remission. The purpose of this study was to further characterize the nature of the Th2 bias in 127-hi cells. Single cell RNA sequencing paired with TCR sequencing of sorted 127-hi memory cells identifies clonally expanded Th2 clusters in 127-hi cells from T1D, but not from healthy donors. The Th2 clusters express GATA3, GATA3-AS1, PTGDR2, IL17K3, IL4R and IL9R. The existence of 127-hi Th2 cell clonal expansion in T1D suggests that disease factors may induce clonal expansion of 127-hi Th2 cells that prolong partial remission and delay disease progression.

Key words: T cells, Th1/Th2, autoimmunity, transcriptome

1. Introduction

Type 1 diabetes (T1D) is an autoimmune disease resulting in the destruction of insulin secreting β -cells by T cells (1). There is no cure for T1D, but several immunotherapies have shown promise (2-5) thereby encouraging the notion that the disease might be reversed by modulating the immune system. Soon after diagnosis, most T1D patients experience a period of reduced insulin requirement (6-9). This period of partial remission can last from several weeks to over a year (10-11). The mechanism of partial remission is not known, but a longer remission period is associated with a reduced risk of acute and long-term T1D complications (12). Partial remission is also associated with better residual β -cell function (6-9) and consensus in the field is that immunotherapy is most effective during this period (2-5).

The mechanism of partial remission is not known. However, previously published work showing that patients with the highest frequency of 127-hi cells have the longest partial remission and greatest C-peptide preservation suggest an immune involvement (13-14). In addition, T1D patients with higher than the mean frequency of 127-hi cells at diagnosis respond more favorably to the anti-inflammatory drug, Abatacept, in the TIDAL clinical trial (14-17). 127-hi cells are a mix of naïve, central memory and effector memory cells, the majority of which are either committed Th2 (14, 18-19), expressing the Th2 transcription factor GATA3 (20), or pre-committed Th2 (14, 18-19) expressing the chemokine receptor CCR4 but not CXCR3 and CXCR5 (21-22).

Th2 cells have been shown to exert a protective effect in the well-established NOD mouse model for spontaneous T1D by secreting the cytokine IL-4 (20, 23). IL-4 negatively influences the

development and expansion of potentially pathogenic pro-inflammatory Th1 cells and their CD8 T cell counterpart, Tc1 cells (24-29). In addition, the Th2-type transcription factor GATA-3 (30) plays a critical role in promoting the Th2 response and in inhibiting Th1 differentiation (31-34). Th1 cells, on the other hand, negatively influence the expansion of Th2 memory cells and are positively induced by cytokines IL-12 and IFN- γ (24-29). These data are consistent with the notion that 127-hi cells play an active role in prolonging length of remission (LoR) and β -cell survival by inhibiting the expansion of pathogenic Th1 and Tc1 cells, because they are predominantly Th2 memory cells. Further characterization of the 127-hi cell population is necessary to determine whether they play a role in protection from T1D progression and whether they can be exploited to reverse and stop the disease. The purpose of this study was to identify the cell subsets and molecular markers within the 127-hi cell compartment that contribute to the Th2 bias.

2. Methods

2.1 Patient population: T1D PBMC for experiments described in Figures 1 and 2 were provided by the Immune Tolerance Network (ITN) (Supplemental Table 1). For Figure 3, PBMC samples were stained at ITN and flow cytometry data sent to SDBRI for analysis (Supplemental Table 2). The flow data in Figure 3 were blinded until after flow cytometry analysis of cell subset frequency was complete and the data were submitted to ITN to be locked. ITN unblinded the data for SDBRI investigators and provided the insulin dose, HbA1c, and C-peptide levels, at either 3 or 6 monthly intervals for at least 2 years, for SDBRI investigators to determine correlations between cell subset frequency and LoR. For the experiments described in Figures 4, 5 and 6, T1D PBMC were made available by ITN for assays performed at SDBRI. SDBRI

investigators are still blinded to age, sex, demographics, and clinical data including insulin dose, HbA1c and C-peptides because this is part of an ongoing much larger study that is still blinded.

2.2 Healthy subject population: For the experiments described in Figures 1, 2, 4, 5 and 6 whole blood from healthy donors was obtained by SDBRI from the Normal Blood Donor Program at The Scripps Research Institute (TSRI) (Supplemental Table 1 for Figures 1 and 2; Supplemental Table 3 for Figures 4, 5 and 6). Human Subjects protocols and consent forms were reviewed and approved by both TSRI IRB and SDBRI IRB. Whole blood was collected in heparin and processed within 2 hours. PBMC were isolated using standard methods and frozen in liquid nitrogen.

2.3 Study approval All clinical investigation was conducted according to Declaration of Helsinki principles. All data involving T1D donors and reported in Figures 1, 3, 4-6 and Tables 1-3, and Supplemental Figures 1-3 and 5, and Supplemental Tables 1, 3-7 of this study were generated at SDBRI using vials of frozen PBMC samples obtained from ITN as part of their prior studies. For the data presented in Figure 5 and Supplemental Figure 4 PBMC samples were labeled for flow cytometry by Benaroya Research Institute and the data analyzed at SDBRI. All ITN human studies were approved by the appropriate Institutional Review Boards and written informed consent was received from participants prior to inclusion in the study. PBMC and data from healthy donors were collected at SDBRI under an approved IRB. The sample use and data analysis for T1D and healthy donor samples was approved by the San Diego Biomedical Research Institute IRB under Exemption 4.

2.4 Measurement of partial remission and β -cell function using IDAA1c and C-peptide AUC: A standard formula, $\text{HbA1c (\%)} + (4 \times \text{insulin dose (U/kg per 24 hours)})$, is used to take into account both insulin requirement and HbA1c levels in a single value, the Insulin Dose Adjusted A1c (IDAA1c). An IDAA1c equal to or less than 9 indicates the partial remission period (35). In this study the end of partial remission is between the last visit when IDAA1c is equal to or less than 9 and the first visit when IDAA1c is greater than 9. Length of remission is the time between diagnosis and end of remission. Stimulated C-peptide AUC was calculated over 120 minutes using the trapezoidal rule, with observed C-peptide values at 0, 15, 30, 60, 90, and 120 minutes. Fasting C-peptide was measured in pmol/mL.

2.5 T cell subsets identified by Flow Cytometry: Vials of PBMC from patients with T1D were thawed and stained at Benaroya Research Institute with the antibody panel, CD3, CD4, CD45RA, CD45RO, CD127, CD25, CCR7, CXCR5, CXCR3 and CCR4, and the flow cytometry data analyzed at SDBRI. This antibody panel was used to identify CD4⁺, CD4⁺ CD25⁺ CD127^{hi} (127-hi), CD4⁺ CD25⁻ (CD25-neg) T cells and Tregs (CD25⁺ CD127^{low}). To quantify the relative frequency of naive (CD45RA⁺, CD45RO⁻, CCR7⁺), central memory (CM; CD45RA⁻, CD45RO⁺, CCR7⁺), and effector memory (EM; CD45RA⁻, CD45RO⁺, CCR7⁻) in total CD4⁺, 127-hi and CD25-neg anti-CCR7, anti-CD45RA and anti-CD45RO antibody staining was also used. To identify pre-committed Th1 and Th2 memory cell subsets within CD4⁺, 127-hi and CD25-neg memory cell populations, CD45RO, CXCR5, CXCR3, and CCR4 staining was used (CD45RO⁺ CXCR5⁻ CXCR3⁺ CCR4⁻ for pre-committed Th1, and CD45RO⁺ CXCR5⁻ CXCR3⁻ CCR4⁺ for pre-committed Th2) (21-22). Data were acquired on an LSRII (ITN), Canto II

(SRSI), LSR Fortessa and LSR II (MCW) and Fortessa X20 (UQ) and analyzed using FlowJo version 10 (Ashland, OR). Isotype or FMO controls were used in every experiment.

2.6 Bulk RNAseq: Healthy and T1D PBMC were thawed and rested overnight. Rested cells were negatively selected for the CD4 subset and stained with fluorescently labeled antibodies specific for CD45RO, CD127 (IL7R), CD25 (IL2RA), and CD3 for cell sorting. 127-hi and CD25-neg memory cells, defined as memory based on their expression of CD45RO, were sorted using an Aria II, RNA was extracted using the Qiagen RNA extraction kit, SMART-Seq® v4 Ultra® Low Input RNA Kit for Sequencing (Takara, Catalog# 634882) and used to generate cDNA. RNASeq was performed at University of California at San Diego Institute of Genomic Medicine (IGM) Sequencing Core and the data was analyzed by UCSF's Center for Computational Biology & Bioinformatics (CCBB). Raw data was analyzed using the Ingenuity Pathway analysis (IPA, Qiagen) software to determine the pathways associated with differentially expressed genes between the 127-hi and CD25-neg memory cell pathways in T1D and healthy donors.

2.7 scRNASeq with paired TCRseq: 127-hi and CD25-neg memory cells were sorted from T1D and healthy PBMC as described above. The sorted cells were counted and processed using 5' reagent kits from 10X Genomics for Single Cell Immune Profiling and TCR Amplification. 5' end sequencing allowed for TCRseq. The number of cells processed was between 5,415 - 10,732 for 127-hi T1D, between 6,521 - 12,279 for CD25-neg T1D, between 2,437 - 8,649 for 127-hi Healthy, and between 4,319 - 8,006 for CD25-neg Healthy (Supplemental Table 7). Gel Beads-in-emulsion (GEM) generation and library preparation was completed as per manufacturer's instructions. Briefly, barcoded gel beads, labeled cells, and partitioning oil were loaded onto a

chromium controller for GEM generation. This process lysed cells and released barcoded primers from gel beads at single cell resolution (within their respective GEM). GEMs were then incubated to produce barcoded cDNA through reverse transcription of mRNA. After cDNA amplification, gene expression and TCR libraries were constructed separately from the same cells. Prior to TCR library construction, full length barcoded V(D)J segments were enriched with two additional PCR amplification steps, using primers specific to the TCR constant region. Once cDNA amplicons were optimized via enzymatic fragmentation and size selection, gene expression libraries were constructed through End Repair, A-tailing, Adaptor Ligation and Sample Index PCR. Sample quality control (QC) and quantification of cDNA and libraries was completed using Qubit 4 fluorometer and Agilent TapeStation 4150. Sequencing of gene expression libraries (25,000 copies for gene expression and 5,000 copies for TCR) was completed at the UCSD IGM, and the Florida State University (FSU) sequencing core facilities.

Data analysis: FASTQ files were uploaded to the 10X genomics Cloud and processed with Cell Ranger V7.0.1 to align reads to the reference genome GRCh38, quantify reads, and create output files. Various output files were then merged for analysis as described for each experiment. Clustering and differential gene expression were completed in Loupe Browser (v6.3.0). All samples were analyzed for mitochondrial gene expression, and number of genes per barcode. High mitochondrial gene expression and lower than expected numbers of genes expressed per barcode can reflect poor quality cells, while unexpectedly high numbers of genes expressed per barcode can reflect multiplets. Thresholds were set at, less than 10% mitochondrial gene expression, and between 500 and 5,000 genes expressed per cell for high quality singlets. For all individual samples analyzed, greater than 99.5% contained less than 10% mitochondrial genes, using GRCh38/hg19 as the reference, indicating high quality viable cells (Supplemental

Table 7). In addition, in more than 99% of each sample the number of genes expressed per barcode was within the expected maximum of 5,000 and minimum of 500 for resting PBMC (36) strongly suggesting high quality singlets (Supplemental Table 7).

2.8 Statistics: Differential gene expression (DGE) of bulk RNAseq data for 127-hi memory cells compared to CD25-neg memory cells was calculated using local false discovery rate (lfdr) also known as the q-value. Genes with less than a lfdr value of 0.3 were considered significant. Associations between T cell subsets and LoR was assessed using Pearson 2-tailed correlation. Significant trends were measured using One-way ANOVA with Multiple Comparison. * indicates a p value of 0.05-0.01. Correlations between levels of expression of genes with T cell subset frequency was determined using Pearson Correlations. Chi-squared (and Fisher's exact) test was used to analyze the Inverse Simpson's Index calculated for all T1D and Healthy clusters to determine whether the clonotypes larger than 20 clones in Th1, Th2 and Th17 clusters are preferentially expanded. All analyses were performed with Graphpad Prism. A p value of less than 0.05 is considered statistically significant.

3. Results

3.1 Th2 bias in 127-hi cells of both healthy and T1D subjects

127-hi memory cells are phenotypically predominantly Th2 (13-14, 19). The remaining, non-Th2, 127-hi cells are mainly either committed Th1 cells (T-bet⁺ IFN- γ ⁺), or pre-committed Th1 cells (CXCR3⁺ CCR4⁻ CXCR5⁻), or Th17 cells (ROR γ t⁺ IL-17⁺) (13-14, 18-19). 127-hi cells also have a functional Th2 bias in that they secrete significantly more IL-4, IL-13, IL5 and IL-10 than

other CD4⁺ memory cells (13-14). CD4⁺ memory cells that do not express CD25 (CD25-neg) also contain pre-committed and committed memory Th1 and Th2 cells and therefore serves as an ideal control cell population to compare 127-hi memory cells and other memory cells (Supplemental Figure 1). To characterize the molecular nature of 127-hi cells, and in particular the Th2 bias, the transcriptome of 127-hi memory cells sorted from Healthy donors and from T1D PBMC samples collected at baseline (within three months of diagnosis) was compared to CD25-neg memory cells sorted from the same donors (Supplemental Figure 2) using bulk RNAseq-derived DGE. 244 genes in Healthy (149 upregulated and 95 downregulated) and 458 genes in T1D (269 upregulated and 189 downregulated) were significantly differentially expressed. Compared to CD25-neg memory cells, 127-hi memory cells in both Healthy and T1D, upregulate several Th2 associated genes including IL17RB (IL-25R, signaling through which promotes Th2 cytokines (37-40)), PTGFR2 (CRTH2 which is involved in secretion of Th2 cytokines IL-4, IL-5 and IL-13 (41-43)), IL9R (IL-9R signaling can support Th2 polarization (44)) and IL2RA (CD25, also associated with IL-4 expression (45-46)). (Figure 1A). Significantly upregulated genes in 127-hi memory cells also include IL4R and GATA3 (Figure 1A). Downregulated genes include GZMK, which promotes pro-inflammatory responses, (47) and EOMES, a transcription factor closely related to T-bet which induces the Th1 cytokine IFN- γ (48) (Figure 1A). These data are consistent with our previously published findings that the dominant functional cell subset within the 127-hi cell population compared to CD25-neg memory cells, in both T1D and Healthy, is Th2.

RNAseq data for all 458 T1D and 244 Healthy genes that were significantly differentially expressed between 127-hi and CD25-neg memory cells (from Figure 1A) were uploaded into the

IPA software and analysis was run to identify key pathways. Within the top ten pathways in 127-hi compared to CD25-neg memory cells in both Healthy and T1D are several Th2-related pathways, including the Th2 pathway, Th1/Th2 activation pathway, T helper cell differentiation, and STAT3 and PI3K/Akt signaling (Figure 1B and C). In addition, the JAK1/JAK3 cytokine signaling pathway is prominent in 127-hi memory cells in T1D (Figure 1B). Analysis of the genes in each of the pathways in 127-hi memory cells compared to CD25-neg cells reveals a significant upregulation of Th2-associated genes and downregulation of Th1-associated genes in both T1D and Healthy (Supplemental Table 4).

The same data from T1D and Healthy donors were analyzed using the String application in the Cytoscape software to determine whether there are gene interactions that are significantly up and down regulated in 127-hi cells. For both T1D and Healthy, the data reveals interactions between upregulated Th2-associated genes, ITGDR2, IL17RB, IL9R and IL2RA (red) and downregulated Th1-associated genes, FCME5 and GZMK (blue). Interactions are also evident between the Th2- and Th1-associated genes and the follicular helper T cell (Tfh) marker CXCR5 and the regulatory marker ICIT, which are also downregulated (Figure 1D for T1D and Supplemental Figure 3 for Healthy).

3.2 Transcriptional circuitry of 127-hi memory Th2 cells differs from CD25-neg memory Th2 cells

To identify genes within 127-hi memory cells that are related to frequency of 127-hi Th2 cells in T1D at baseline, the level of expression of all differentially expressed genes in T1D 127-hi compared to CD25-neg memory cells (458 genes) was correlated with the frequency of 127-hi

Th2 and CD25-neg Th2 cells within the total CD4⁺ T cell compartment of T1D sorted populations used for RNAseq. The top 25 positive and top 25 negative correlates with 127-hi Th2 cell frequency are shown in Figure 2A (left panel). Correlations between the same expressed genes with CD25-neg Th2 cell frequency are shown for comparison (Figure 2A, right panel). PRDM1 (encodes Blimp-1) a transcriptional repressor of T-bet and IFN- γ (50-51), LRRFIP1 a transcription repressor of the inflammatory cytokine TNF- α (52-53), and the Th2 marker CCR4 positively correlate with the frequency of 127-hi Th2 cells (Figure 2B) but not CD25-negTh2 cells (Figure 2C). In contrast, ZBTB16, a transcription factor for Th17 cells (54), and TIGIT, negatively correlate with 127-hi (Figure 2B) but positively correlate with CD25-neg Th2 cells (Figure 2C). In addition, the level of expression of IL12RB2, the IL-12 receptor, which is a driver of Th1 responses (55-56), negatively correlates with the relative frequency of 127-hi (Figure 2B) but not CD25-neg Th2 cells (Figure 2C), while IL6ST, also a driver of pro-inflammatory Th1 cells (56) negatively correlates with both 127-hi and CD25-neg Th2 cells (Figure 2B and C). These data overall support the hypothesis that the frequency of 127-hi Th2 and CD25-neg Th2 cells in T1D is influenced by different molecular pathways.

3.3 The frequency of 127-hi Th2 EM cells positively correlates with LoR

Based on the cumulative findings that 127-hi memory cells are highly Th2-like compared to other memory CD4 T cells, we tested the hypothesis that 127-hi Th2 memory cells correlate with LoR. To that end, twenty-six pediatric T1D PBMC samples collected at baseline were analyzed for relative frequencies of 127-hi and CD25-neg Th1 and Th2 cell subsets within the total CD4⁺ T cell compartment and correlations between cell subset frequencies and LoR determined. Participant information is summarized in Supplemental Table 2. There is a significant correlation

between LoR and the frequency of 127-hi Th2 EM and CD25-neg Th2 EM cell frequency, but significance is stronger for the former (Figure 3A, $p = 0.003$ compared to $p = 0.03$). Th1 and CM cell subsets do not correlate significantly with LoR (Figure 3A). The frequency of both 127-hi and CD25-neg Th2 EM cells (Figure 3B and C respectively), but none of the other cell subsets tested (Supplemental Figure 4), significantly decline between 3 and 12 months post-baseline. As expected, during the same time-period, IDAA1c increases (Figure 3D) while C-pep AUC decreases (Figure 3E) indicating a decline in β -cell function and disease progression between diagnosis and 12 months post-baseline. However, the frequency of either 127-hi Th2 EM, or CD25-neg Th2 EM does not correlate significantly either negatively with IDAA1c, or positively with C-pep AUC (data not shown).

3.4 127-hi Th2 cells differ transcriptionally from other Th2 cells

To directly test whether memory 127-hi and CD25-neg Th2 cells are different, scRNAseq was performed on memory 127-hi and CD25-neg memory cells sorted from healthy ($n=4$) and T1D ($n=7$) PBMC. In a first analysis, the transcriptomes of all seven T1D 127-hi samples were merged and compared to the merged transcriptomes of all seven T1D CD25-neg samples. Similarly, the transcriptomes of all four Healthy 127-hi samples were merged and compared to the merged transcriptomes of all four Healthy CD25-neg samples. Th2 and Th1 cells were identified using the expression of Th2 (PTGDR2, IL17RB, IL9R, HPGDS and GATA3-AS1 shown in blue) and Th1 (EOMES, GZMA, GZMK, TBX21, IFNG, IFNG-AS1, IL12RB shown in orange) associated genes (Supplemental Figure 5). In both T1D (Supplemental Figure 5A) and Healthy (Figure 5B), the frequency of Th2 (blue) cells is higher in 127-hi cells than CD25-neg

cells whereas the frequency of Th1 cells (orange) is lower, consistent with data generated in bulk RNAseq (Figure 1).

To evaluate the contribution of each individual sample to the combined transcriptome the remaining analysis was performed on each of the seven T1D and four Healthy samples separately. The many clusters identified in tSNE plots from individual samples indicates that 127-hi and CD25-neg memory populations are extremely heterogeneous in both T1D (Figure 4A and B and Supplemental Figure 6E-J) and in Healthy (Supplemental Figure 6A-D). In addition, in both T1D and Healthy samples, some clusters are almost entirely either 127-hi or CD25-neg indicating that the 127-hi memory cell population contains cell subsets that are absent from CD25-neg memory cells and vice versa (Figure 4C-D).

DGE was used to identify clusters that represent committed Th1, Th2 and Th17 cells by comparing each cluster in each sample with all other clusters (Table 1). Of the seven T1D samples, three had clusters with upregulated Th2 cell subset specific markers GATA3 and GATA3-AS1, as well as PTC2R2, IL17RB, IL9R, HPGDS, IL4R, and downregulated CCR7 indicating Th2 EM clusters (Table 1A). Four T1D samples had clusters with upregulated EOMES, the transcription factor for non-classical Th1, as well as GZMA and GZMK, indicating a cytotoxic phenotype. In some of these Th1 clusters IFNG, IFNG-AS1, CXCR3, IL12RB2 and the classical Th1 transcription factor, TBX21 were also upregulated. Also, four T1D samples had clusters with upregulated expression of the Th17 marker RORC (57) and two of these clusters also had upregulated CCR6 and ZBTB16. Unlike the Th2 clusters, Th17 clusters upregulated CCR7 indicating CM status. Healthy samples contained Th1 and Th17 clusters, but not Th2

(Table 1A). Moreover, the Th2 and Th17 clusters identified by DGE are greater than 90% 127-hi, whereas the Th1 clusters are either greater than 90% CD25-neg, or a mix of 127-hi and CD25-neg (Table 1A). These data are consistent with previously published data that show a Th2 bias in the 127-hi cell population compared to CD25-neg in T1D.

As another approach to determine the Th1, Th2 and Th17 cluster types, the DGE data for all clusters in each sample were imported into the Ingenuity Pathway Analysis (IPA) software. Clusters with a significant upregulation of the Th1 pathway, Th2 pathway and Th17 pathway (z-score equal to or greater than 2) were considered indicators of Th1, Th2 and Th17 clusters respectively (Table 1B). Using this approach, all five Th2 clusters and one Th1 cluster previously identified by DGE were also identified using IPA (shown in parenthesis in Table 1B). Also, several additional Th1 and one additional Th2 clusters were identified. Analysis of the genes used by IPA to identify each Th2 cluster revealed that GATA3, PTGDR2, IL17RB and IL4R were again routinely upregulated. In addition, two of the Th2 clusters had significant downregulation of the Th1-associated gene, IL12RB2. Of the ten Th1 clusters identified by IPA, nine expressed high levels of MHC Class II, only one expressed the Th1 transcription factor TBX21, and none expressed EOMES (Table 1B). All Th1 and Th2 clusters identified by IPA were also evaluated for involvement of additional pathways. Additional pathways in the Th2 clusters include IL-4, STAT3, and TCR signaling pathways. Th1 clusters also had consistent upregulation of TCR and IL-4 signaling, with downregulation of IL-10, CTLA4, Th2, PD-1-PDL-1 pathways (Table 1B).

The Th1 and Th17 clusters that were identified by DGE (Table 1A) but not by IPA (Table 1B) were also evaluated for involvement of additional pathways using IPA (Supplemental Table 5). TCR and, surprisingly, IL4 signaling was elevated and CTLA4 signaling downregulated in two Th1 clusters. No additional pathways were identified for the remaining Th1 clusters. Five of the six Th17 clusters had combinations of upregulated IL-6, CTLA4 and PD-1-PDL-1 pathways and down regulation of the TCR pathway (Supplemental Table 5).

3.5 Preferential TCR gene usage in Th2 cells in individuals with T1D

An active role for Th2 EM cells in partial remission would most likely involve their proliferation which, if substantial enough, could be visualized by preferential TCR gene usage and clonal expansion. As a first step, we used the transcriptomic data already generated to screen all T1D and Healthy samples for the preferential expression (upregulation) of genes that encode TCR V β and V α gene segments compared to all other clusters by DGE. In the T1D sample shown (Figure 5A), TRBV5-4 and TRAV8-1 genes are expressed in 127-hi but not in CD25-neg clusters. Gene expression analysis of Th2-associated genes shows that the expression of GATA3, GATA-AS1, IL9R, PTGDR2 and IL4R coincides with the TRBV5-4 and TRBV8-1 positive clusters. The same cell clusters do not express CCR7, consistent with EM cells (Figure 5B). Five of the seven T1D and all the four Healthy samples analyzed have preferential expression of at least one TCR gene segment in at least one cluster, including clusters that were previously identified as Th2, Th1 and Th17 clusters (Table 2). Preferential TCR gene usage was also seen in Th1 cell clusters in Healthy samples.

3.6 Clonal expansion and co-localization with cell types using paired single cell TCR sequencing and scRNAseq

Clonotypes (groups of cells with identical TCR) were identified in each T1D and Healthy, 127-hi and CD25-neg sample by matching identical TCR V β , V α and CDR3 amino acid sequences. Using Loupe Browser the number of clones in each clonotype were counted. Clonotypes with 20 or more clones were co-located with clusters, including those previously identified as Th1, Th2 and Th17 cell types, by pairing TCR sequencing with the transcriptome data.

The total number of clonotypes in all 127-hi T1D samples was 29, which far exceeded the total number of clonotypes in CD25-neg cells (n=8) from the same samples (Supplemental Table 6A and B). In contrast, the total number of clonotypes in all 127-hi Healthy samples was less (n = 5) than the total number of clonotypes from CD25-neg cells (n = 13) from the same individuals (Supplemental Table 6C and D). In most cases, for both 127-hi and CD25-neg cells, individual clonotypes were predominantly restricted to one or two clusters. However, in some cases single clonotypes were evident in several clusters. In addition, many clusters contained several clonotypes (Figure 6A and Supplemental Figure 6A-J).

Co-location of clonotypes with cell types revealed clonal expansion (clonotypes with more than 20 clones) in all T1D 127-hi clusters previously identified as Th2 by either DGE or IPA (Table 3 and Supplemental Figure 5). Moreover, clonally expanded T cell co-expressed Th2-associated genes, GATA3, IL9R and PRGDR2 confirming clonal expansion of Th2 cells (Figure 6B-D). These data indicate that 127-hi Th2 cells can clonally expand in some T1D individuals at or before diagnosis. Evidence of clonal expansion was also detected in T1D Th1 and Th17 clusters. In Healthy samples, clonal expansion was evident in Th1 clusters (Table 3 and Supplemental Figure 5). To determine whether clonal expansion was more prevalent in Th2,

Th1 and Th17 clusters compared to all other clusters the TCR repertoire diversity of each cluster in both T1D and Healthy samples (a total of 135 clusters) was calculated using Inverse Simpson's Index (ISI), where lower numbers reflect a lower the level of diversity and higher level of clonal expansion. Of 13 clusters that have an ISI equal to or lower than 500 (Figure 6E), 11 were previously identified as either Th2 or Th1 (5 T1D Th2, 2 T1D Th1 and 4 Healthy Th1). Out of the remaining 122 clusters, only 2 had an ISI less than 500. One of these was a T1D Th1 cluster and the other a Healthy cluster of unknown cell type. Analysis of the data indicates that the distribution of clonal expansion is not equivalent in all clusters and that clonal expansion in some Th2 and Th1 clusters is significantly higher than in other clusters (Chi-square, $p < 0.0001$). Overall, the data confirm a high level of clonal expansion in both Th2 and Th1 clusters in T1D and in Th1 clusters in Healthy (Figure 6E).

To date none of the clonotypes identified in T1D have been found in other individuals in this study and no matches have been found within the mc-PAS-TCR or nPOD TCR/BCR SEARCH data bases. Of all the Healthy clonotypes identified, 1 match was found in the mc-PAS-TCR data base and that was in Healthy #1, specific for M.Tuberculosis, indicating that this clone is public (present in more than one individual).

In T1D, although both Th1 and Th2 clonal expansion is evident, the Th2 clonotypes are generally larger (contain more clones) than the Th1 clonotypes and individual Th2 clusters contain several different expanded clonotypes whereas Th1 clusters have only a single expanded clonotype suggesting less diversity in the Th1 response (Table 3). In Healthy samples, clonal expansion of multiple clonotypes is detected in both classical and non-classical Th1 clusters (Table 3).

4. Discussion

T1D is a progressive autoimmune inflammatory disease. After diagnosis, glucose control continues to decline as destruction of the insulin secreting β -cells continues. Glucose control can be quantified by combining HbA1c levels and daily exogenous insulin intake to measure insulin dose adjusted A1c, IDAA1c. Patients with an IDAA1c of 9 or lower are in a state of transient partial remission. Our group has previously shown that the LoR, which is the period between diagnosis and the time when IDAA1c is above 9, and β -cell survival, correlates with the frequency of CD4 T cells that express CD25 and CD127 (127-hi cells) at diagnosis (13-14). 127-hi cells are a mix of naïve and memory cell subsets with a bias towards Th2 memory cells (14, 19). In the current study, we show that within the 127-hi cell population it is the Th2 EM cells that correlate with LoR. Analysis of the 127-hi memory cell transcriptome reveals significantly higher levels of Th2-associated genes *ITGDR2*, *IL17RB*, and *IL9R* and lower levels of inflammatory genes, *IL12RB2*, *EOMFS* and *GZMK* than the remaining CD4⁺ memory cells (CD25-neg cells) in both healthy and T1D PBMC samples. In single cell RNA sequence analysis clusters with a committed Th2 EM profile are identified in T1D 127-hi cells but not CD25-neg cells. The T1D 127-hi Th2 EM clusters contain multiple expanded clonotypes suggesting that the clusters might develop from the clonal expansion of Th2 cells. Unexpectedly, in T1D, clonal expansion of Th2 cells is more common than clonal expansion of Th1 cells. The existence of 127-hi Th2 EM cell clonal expansion in T1D, coupled with the finding that the best CD4 T cell correlate with LoR is 127-hi Th2 EM cell frequency, suggests that the presence of T1D can induce clonal expansion of 127-hi Th2 EM cells that promote protection to prolong partial remission and delay disease progression.

Correlation analysis between the frequency 127-hi Th2 cells and levels of gene expression in the sorted cell populations supports the idea that the mechanism(s) that control 127-hi Th2 frequency are likely to involve down regulation of Th1 and other inflammatory genes. Thus, PRDM1, a transcription repressor of T-bet and IFN- γ (49-50), and LRRFIP1, a transcription factor for TNF- α (52-53) are both expressed at higher levels in sorted populations with the highest frequency of 127-hi Th2 cells, whereas IL12RB2 (54-55) and IL6ST (55), both drivers of inflammatory responses, are expressed at low levels in the same samples. However, this is not the case for CD25-neg cells supporting the hypothesis that 127-hi and CD25-neg Th2 cell frequency is under the control of different molecular pathways. There are several other mechanisms that might control the frequency in 127-hi cells in T1D. 127-hi cells express a high density of CD44v6 (13), a receptor for high molecular weight hyaluronan (HA). During inflammation, low molecular forms of hyaluronan (HA) that are generated during inflammation can bind but not cross-link CD44v6 and fail to inhibit apoptosis by mechanisms that are dependent on CD44v6 signaling (59-62). In addition, soluble CD127 and CD25 receptors (sCD127R and sCD25R) that are released from activated T cells during inflammation can act as IL-7 and IL-2 antagonists, potentially blocking IL-7 and IL-2 mediated signaling and the expansion and survival of 127-hi cells (63-65).

Several genes that are differentially expressed in 127-hi memory cells compared to CD25-neg memory cells are known putative candidate genes for T1D associated GWAS loci, including IL2RA, IL12RB2, JAK1 and JAK3 (66). Thus, IL2RA is upregulated and IL12RB2 downregulated in 127-hi memory cells, and JAK1 and JAK3 are part of the 127-hi memory cell cytokine signaling pathway in T1D. The link between genes that are risk factors for T1D and

their expression in 127-hi Th2 cells supports the idea that 127-hi Th2 cells are mechanistically linked to protecting from disease progression in T1D potentially by deviating responses away from inflammatory Th1/Tc1 responses.

Clonal expansion in CD4 T cells in T1D has been reported extensively for Th1 (67) and these cells are thought to respond to autoantigen and have pathogenic function (67). Clonal expansion of Th2 cells expressing both GATA3 and CCR4 has also been described previously in T1D (68). The clonotypes detected had 4-8 clones per clonotype with one or two Th2 clonotypes in each subject, and the presence of the Th2 clonotypes was thought to be associated with pathology (68). The samples analyzed in the former study were from established T1D (18-28 months post-diagnosis) and this might explain the differences seen between the former study and the one presented here. The extensive Th2 cell clonal expansion described here, with multiple clonotypes and large numbers of clones per clonotype suggests an established and ongoing immune response with possible epitope spreading. The positive correlation between the frequency of 127-hi Th2 cells and LoR, suggests that the 127-hi Th2 responses are induced by T1D, possibly as an attempt, albeit ultimately a failed attempt, to protect from disease progression. Th17 clonotypes, identified by their upregulation of RORC (56), were also seen in 127-hi T1D cells. It is unlikely that these Th17 cell clusters are Th2/Th17 cells previously described in asthma (69-70) as they do not co-localize with the Th2 cell clusters.

Several of the TCR genes that were identified as preferentially used, using DGE, were also present in the clonotypes for T1D 127-hi Th2 (TBV5-4, TRBV4-1, TRBV29-1, TRBV10-2, TRVA8-1, TRAV10, TRBJ2-3), T1D 127-hi Th17 (TRAJ11), T1D CD25-neg Th1 (TRBV7-2,

TRAV38-1, TRBJ2-3), and healthy CD25-neg Th1 (TRBV14, TRBV20-1, TRAV13-2, TRAV34). However, to date, none of the 38 clonotypes found in the T1D group in this study matched autoantigen-specific clonotypes previously described in human T1D (67), and no matches were found in the mc-PAS-TCR and nPOD TCR/BCR SEARCH data bases. Proliferation of CD4 T cells that predicted a longer partial remission has been reported previously in T1D (71). In that study the CD4 T cells were specific for proinsulin (peptide 33-63) but the cell type was not determined (71).

Studies in human and mouse have described several different Th2 cell subtypes (72). Thus, scRNAseq analysis of circulating CD4 memory T cells from people with allergies to house dust mite (HDM) with and without asthma identifies Th2 cell subsets that express GATA3, IL17RB, IL9, GZMB, IL-5, and PPARG in those with asthma and Th2 cells expressing GATA3, IL-4, IL-21, IL1RL1 and ICOS in non-asthmatic individuals (73). Th2 cells isolated from nasal polyps express CRTH2 (encoded by the gene *PTGD2*), IL17RB, and IL1RL1 by flow cytometry and GATA3, IL17RB, IL4, IL9, IL5 and IL13 by gene expression (74). Th2A cells are distinguished from conventional Th2 cells in allergic patients by their co-expression of CRTH2, CD161, CD49d and a low density of CD27 (73-74) with elevated IL-5 and IL-9 measured by flow cytometry, and by their expression of IL17RB, HGPDS, IL1RL1, PPARG, IL9, IL5 and KLRB1 (encodes CD161) in scRNAseq experiments (75-77). Transcriptome comparisons of tissue resident Th2 cells (Trm Th2) isolated from bronchial biopsies from asthmatic donors expressed elevated levels of GATA3, HGPDS, PPARG, IL17RB and IL9R compared to non-asthmatic individuals (78). In the Th2 clusters identified in our current study, IL9, GZMB, IL5, PPARG, IL1RL1, IL4, IL21, or ICOS were not upregulated suggesting that they are not the Th2 cells

previously identified in people with HDM allergy with or without asthma, nor a circulating form of Trm Th2, or Th2 cells from nasal polyps (73). Neither do they express Th2A markers KLRG1 (the gene that encodes CD161) and ITGA4 (the gene that encodes CD49d). Instead, the 127-hi Th2 EM cells have a non-pathogenic anti-inflammatory cell phenotype that is consistent with a role in actively prolonging LoR and delaying disease progression.

The existence of clonally expanded anti-inflammatory Th2 cells within the 127-hi cell population in people newly diagnosed with T1D might suggest a naturally occurring mechanism of protection, that manifests itself by delaying the end of the partial remission period. Therapeutic strategies to expand 127-hi Th2 cells might benefit people with T1D by promoting, extending and enhancing the remission period. An enhanced remission period might, in turn, lead to a reduction in long-term complications, development of a permissive environment for current immunotherapies, and in some cases, reverse T1D.

5. Conclusion

Both the cellular and molecular data presented in this study indicate that the correlation between 127-hi cells and LoR involves clonal expansion of the 127-hi Th2 EM cell subset. The study also sheds light on 127-hi Th2 EM molecular targets and pathways that might be exploited to promote their function and frequency. These data might be used to extend the remission period, delay disease progression and identify biomarkers to predict disease progression and response to treatment.

6. Acknowledgements

A.N. generated the data, prepared data for all Figures and Tables, contributed to data analysis and to the writing of the manuscript. With A.N., F.A. generated scRNAseq/TCRseq data. A.N. and B.L. generated and analyzed the bulk RNASeq data. T.T. and D.S. contributed to flow cytometry data analysis, B.L. contributed to bulk RNAseq data analysis and A.V. contributed to scRNAseq/TCRseq data analysis. S.A.L. coordinated the flow cytometry staining for the study in Figure 3. L.C. coordinating the selection, blinding and transfer of T1D PBMC samples from ITN to SDBRI. E.S. coordinated the collaboration between ITN and SLPRI for the study in Figure 3 and contributed to the design of the antibody panel for that study. ITN provided samples and clinical data. J.D.D. designed the research study, coordinated the collaborative team, samples and data. J.D.D. also contributed to data analysis and wrote the manuscript. We would like to thank Drs. Lauren Higdon and Srinath Sanda (ITN, San Francisco, California, U.S.A.) for reading and making comments on the manuscript, and Dr. Sara Brin Rosenthal from the Center for Computational Biology and Bioinformatics (CCBB) at the University of California, San Diego (UCSD), for TCR sequence match searches using the mc-PAS-TCR and nPOD TCR/BCR Search databases. We also thank Sanford Burnham Prebys Flow Core facility for troubleshooting and conducting the sort on the bulk RNASeq samples, the Human Embryonic Stem Cell Core (HESCCF) Facility at Sanford Consortium who conducted the cell subset sorting for the scRNASeq samples. This publication includes data generated at the UC San Diego IGM Genomics Center utilizing an Illumina NovaSeq 6000 that was purchased with funding from a National Institutes of Health SIG grant (#S10 OD026929).

7. Funding

Funding for this study was provided by The Leona M. & Harry B. Helmsley Charitable Trust Grant #2207-05421 to JDD. Portions of the research reported in this publication was performed using samples from clinical trials of the Immune Tolerance Network, which is supported by the National Institute of Diabetes and Digestive and Kidney Diseases (NIDDK) and the National Institute of Allergy and Infectious Diseases (NIAID) of the National Institutes of Health under Award Number UM1AI109565. The content is solely the responsibility of the authors and does not necessarily represent the official views of the National Institutes of Health.

8. References

1. Atkinson MA, et al. Type 1 diabetes. *Lancet (London, England)* 2014;383:69–82.
2. Herold KC., et al. A single course of anti-CD3 monoclonal antibody hOKT3gamma1(Ala-Ala) results in improvement in C-peptide responses and clinical parameters for at least 2 years after onset of type I diabetes. *Diabetes* 2005;54:1763-1769.
3. Keymeulen BE, et al. Insulin needs after CD3-antibody therapy in new-onset type I diabetes. *N Engl J Med* 2005;352:2598-2608.
4. Keymeulen BM. et al. Four-year metabolic outcome of a randomized controlled CD3-antibody trial in recent-onset type I diabetic patients depends on their age and baseline residual beta-cell mass. *Diabetologia* 2010;53:614-623.
5. Sherry, N., W. et al. Protégé Trial Investigators. Teplizumab for treatment of type I diabetes (Protégé study): 1-year results from a randomized, placebo-controlled trial. *Lancet* 2011;378:487-497.
6. Keymeulen B, Somers G. Immunointervention in type 1 (insulin-dependent) diabetes mellitus. *Acta Clin Belg* 1993;48:86-95.

7. Muhammad BH, et al. Partial remission phase of diabetes in children younger than 10 years. *Arc Dis Child* 1999;80:367-369.
8. Bober EB, et al. Partial remission phase and metabolic control in type I diabetes mellitus in children and adolescents. *J Pediatr Endocrinol Metab* 2001;14:435-441.
9. Buyukgebiz A, et al. Factors influencing remission phase in children with type I diabetes mellitus. *J Pediatr Endocrinol Metab* 2001;14:1585-1596 .
10. Lombardo F, et al. Two-year prospective evaluation of the factors affecting honeymoon frequency and duration in children with insulin dependent diabetes mellitus: the key-role of age at diagnosis. *Diabetes Nutr Metab* 2002;15:246-251.
11. Abdul-Rasoul M, et al. 'The honeymoon phase' in children with type I diabetes mellitus: frequency, duration, and influential factors. *Pediatr Diabetes* 2006;7:101-107.
12. Steffes MW, et al. Beta-cell function and the development of diabetes-related complications in the diabetes control and complications trial. *Diabetes Care* 2003;26:832-836.
13. Moya R, et al. A pilot study showing associations between frequency of CD4⁺ memory cell subsets at diagnosis and duration of partial remission in type 1 diabetes. *Clinical Immunology* 2016;166:72-80.
14. Narsale A, et al. CL⁺CD25⁺CD127^{hi} cell frequency predicts disease progression in type 1 diabetes. *JCI Insight* 2021;6:e136114.
15. Rigby MR, et al. Targeting of memory T cells with alefacept in new-onset type 1 diabetes (T1DAL study): 12 month results of a randomized, double-blind, placebo-controlled phase 2 trial. *Lancet Diabetes Endocrinol.* 2013;1:284-94.

16. Pinckney A, et al. Correlation Among Hypoglycemia, Glycemic Variability, and C-Peptide Preservation After Alefacept Therapy in Patients with Type 1 Diabetes Mellitus: Analysis of Data from the Immune Tolerance Network T1DAL Trial. *Clin Ther* 2016;38:1327-1339.
17. Rigby MR, et al. Alefacept provides sustained clinical and immunological effects in new-onset type 1 diabetes patients. *J Clin Invest* 2015;125:3285-96.
18. Narsale A, et al. Data on correlations between T cell subset frequencies and length of partial remission in type 1 diabetes. *Clinical Immunology Data in Brief* 2015;8:1348-1351.
19. Narsale A, et al. Human CD4⁺ CD25⁺ CD127^{hi} cells and the Th1/Th2 phenotype. *Clinical Immunology* 2018;188:103-112.
20. Walker LS., von Herrath M. CD4 T cell differentiation in type 1 diabetes. *Clin Exp Immunol* 2016;183:16-29.
21. Rivino L et al. Chemokine receptor expression identifies pre-T helper (Th1), pre-Th2, and nonpolarized cells among human CD4⁺ central memory T cells. *J Exp Med* 2004;200:725-735.
22. Kim CH et al. Rules of chemokine receptor association with T cell polarization in vivo. *J Clin Invest* 2001;108:1331-1339.
23. Turner MS, et al. Low TCR signal strength induces combined expansion of Th2 and regulatory T cell populations that protect mice from the development of type 1 diabetes. *Diabetologia* 2014;57:1428-1436.
24. Abbas AK, et al. Functional diversity of helper T lymphocytes. *Nature* 1996;383:787-793.
25. O'Garra A. Cytokines induce the development of functionally heterogeneous T helper cell subsets. *Immunity* 1998;8:275-83.
26. Paul WE, Seder RA. Lymphocyte responses and cytokines. *Cell* 1994;76:241-51.

27. Szabo SJ, et al. Distinct effects of T-bet in TH1 lineage commitment and IFN-gamma production in CD4 and CD8 T cells. *Science* 2002;295:338–342.
28. Oswald IP, et al. IL-12 inhibits Th2 cytokine responses induced by eggs of *Schistosoma mansoni*. *J Immunol* 1994;153:1707–1713.
29. Gavett SH, et al. Interleukin 12 inhibits antigen-induced airway hyperresponsiveness, inflammation, and Th2 cytokine expression in mice. *J Exp Med* 1995;182:1527–1536.
30. Zhang DH, et al. Transcription factor GATA-3 is differentially expressed in murine Th1 and Th2 cells and controls Th2-specific expression of the interleukin-5 gene. *J Biol Chem* 1997;272:21597-21603.
31. Hwang ES, et al. T helper cell fate specified by kinase-mediated interaction of T-bet with GATA-3. *Science* 2005;307:430-433.
32. Zheng, WP, Flavell RA. The transcription factor GATA-3 is necessary and sufficient for Th2 cytokine gene expression in CD4 T cells. *Cell* 1997;89:587-596.
33. Zhu J, et al. GATA-3 promotes Th2 responses through three different mechanisms: Induction of Th2 cytokine production, selective growth of Th2 cells and inhibition of Th1 cell-specific factors. *Cell Res* 2006;16:3–10.
34. Ouyang W, et al. Inhibition of Th1 development mediated by GATA-3 through an IL-4-independent mechanism. *Immunity* 1998;9:745-755.
35. Mortensen HB et al. New definition for the partial remission period in children and adolescents with type 1 diabetes. *Diabetes Care* 2009;32:1384-1390.
36. Derbois C et al. Single cell transcriptome sequencing of stimulated and frozen human peripheral blood mononuclear cells. *Scientific Data* 2023;10:433-443.

37. Fort MM, et al. IL-25 induces IL-4, IL-5 and IL-13 and Th2-associated pathologies in vivo. *Immunity* 2001;15:985-995.
38. Pan G, et al. Forced expression of murine IL-17E induces growth retardation, jaundice, a Th2-biased response, and multiorgan inflammation in mice. *J Immunol* 2001;167:6559-6567.
39. Tamachi T, et al. IL-25 enhances allergic airway inflammation by amplifying a Th2 cell-dependent pathway in mice. *J Allergy Clin Immunol* 2006;118:606-614.
40. Angkasekwinai P, et al. Interleukin 25 promotes the initiation of proallergic type 2 responses. *J Exp Med* 2007;204:1509-1517.
41. Hirai H, et al. Prostaglandin D2 selectively induces chemotaxis in T helper type 2 cells, eosinophils, and basophils via seven-transmembrane receptor CRTH2. *J Exp Med* 2001;193:255-261.
42. Tanaka K, et al. Effects of prostaglandin Γ 2 on helper T cell functions. *Biochem Biophys Res Commun* 2004;316:1009-1014.
43. Xue L, et al. Interaction between prostaglandin D and chemoattractant receptor homologous molecule expressed on Th2 cells mediates cytokine production by Th2 lymphocytes in response to activated mast cells. *Clin Exp Immunol* 2009;156:126-133.
44. Do-Thi VA, et al. Crosstalk between the producers and immune targets of IL-9. *Immune Network* 2020;20:e45.
45. Zhu J, et al. Stat5 activation plays a critical role in Th2 differentiation. *Immunity* 2003;19:739-748.
46. Cote-Sierra J, et al. Interleukin 2 plays a central role in Th2 differentiation, *Proc Natl Acad Sci USA* 2004;101:3880-3885.

47. Joeckel LT, et al. Mouse granzyme K has pro-inflammatory potential. *Cell Death & Differentiation* 2011;18:1112-1119.
48. Suto A, et al. IL-21 inhibits IFN-gamma production in developing Th1 cells through the repression of Eomesdermin expression. *J Immunol* 2006;177:3721-3727.
49. Seif F, et al. The role of JAK-STAT signaling pathway and its regulators in the fate of T helper cells. *Cell Commun Signal* 2017;15:23-30.
50. Martins GA, et al. Transcriptional repressor Blimp-1 regulates T cell homeostasis and function. *Nature Immunology* 2006;7:457-465.
51. Cimmino L, et al. Blimp-1 attenuates Th1 differentiation by repression of ifng, tbx21 and bcl6 gene expression. *J Immunol* 2008;181:2338-2347.
52. Suriano AR, et al. GCF2/LRRFIP1 represses tumor necrosis factor alpha expression. *Mol Cell Biol* 2005;25:9073-9081.
53. Shi L, et al. Non-coding RNAs and LRRFIP1 regulate TNF expression. *J Immunol* 2014;192:3057-3067.
54. Cheng Z-Y, et al. ZBTB transcription factors: Key regulators of the development, differentiation and effector function of T cells. *Front Immunol* 2021;12:713294
55. Costa V, et al. Distinct antigen delivery systems induce dendritic cells divergent transcriptional response: New insights from a comparative and reproducible computational analysis. *Int J Mol Sci* 2017;18:494
56. Karpus WJ, Kennedy KJ. MIP-1a and MCP-1 differentially regulate acute and relapsing autoimmune encephalomyelitis as well as Th1/Th2 lymphocyte differentiation. *J Leukoc Biol* 1997;62:681-687.

57. Hall JA, et al. Transcription factor ROR α enforces stability of the Th17 effector program by binding to a Rorc cis-regulatory element. *Immunity* 2022;55:2027-2043.
58. Warshauer JT, et al. A human mutation in STAT3 promotes type 1 diabetes through a defect in CD8+ T cell tolerance. *J Exp Med* 2021;218,e20210759.
59. Bollyky PL, et al. High molecular weight hyaluronan promotes the suppressive effects of CD4+ CD25+ regulatory T cells. *J Immunol* 2007;179:744-747.
60. Borland G, et al. Forms and functions of CD44. *Immunology* 1998;93:139-148.
61. Rajasagi M, et al. CD44 promotes progenitor homing into the thymus and T cell maturation. *J Leukocyte Biology* 2008;85:251-261.
62. Ayroldi E L, et al. CD44 (Pgp-1) inhibits CD3 and dexamethasone-induced apoptosis. *Blood* 1995;86:2672-2678.
63. Monti P, et al. Concentration and activity of the soluble form of the interleukin-7 receptor alpha in type 1 diabetes identifies an interplay between hyperglycemia and immune function. *Diabetes* 2013;62:2500-2508.
64. Downes K, et al. Plasma concentrations of soluble IL-2 receptor alpha (CD25) are increased in type 1 diabetes and associated with reduced C-peptide levels in young patients. *Diabetologia* 2014;57:366-372.
65. Yang ZZ, et al. Soluble IL-2R alpha facilitates IL-2-mediated immune responses and predicts reduced survival in follicular B cell non-Hodgkin lymphoma. *Blood* 2011;118:2809-2820.
66. Robertson CC, et al. Fine-mapping, trans-ancestral and genomic analyses identify causal variants, cells, genes and drug targets for type 1 diabetes. *Nature Genetics* 2021;53:962-971.
67. Nakayama M, Michels AW. Using the T cell receptor as a biomarker in Type 1 Diabetes. *Frontiers in Immunology* 2021;12:777788.

68. Cerosaletti K, et al. Single-cell RNA-seq reveals expanded clones of islet antigen-reactive CD4⁺ T cells in peripheral blood of subjects with type 1 diabetes. *J Immunol* 2017;199:323-335.
69. Irvin V, et al. Increased frequency of dual-positive Th2/Th17 cells in bronchoalveolar lavage fluid characterizes a population of patients with severe asthma. *J Allergy Clin Immunol* 2014;134:1175-1186.
70. Liu W, et al. Mechanism of Th2/Th17-predominant and Neutrophilic, Th2/Th17-low Subtypes of Asthma. *J Allergy Clin Immunol* 2018;139:1548-1558.
71. Musthaffa Y, et al. Proinsulin-specific T-cell responses correlate with estimated c-peptide and predict partial remission duration in type 1 diabetes. *Clin Transl Immunology* 2021;10:e1315.
72. Harker JA, Lloyd CM. T helper 2 cells in asthma. *Exp Med* 2023;220:e20221094.
73. Seumois G, et al. 2020. Single-cell transcriptomic analysis of allergen-specific T cells in allergy and asthma. *Sci Immunol* 2020;5:eaba6087.
74. Lam EP, et al. IL-25/IL-33-responsive Th2 cells characterize nasal polyps with a default Th17 signature in nasal mucosa. *J Allergy Clin Immunol* 2016;137:1514-1524.
75. Mitson-Salazar A, et al. Hematopoietic prostaglandin D synthase defines a proeosinophilic pathogenic effector human T(H)2 cell subpopulation with enhanced function. *J Allergy Clin Immunol* 2016;137:907-918.
76. Wambre E, et al. A phenotypically and functionally distinct human Th2 cell subpopulation is associated with allergic disorders. *Sci Transl Med* 2017;9:eaam9171.
77. Luce S, et al. Decrease in CD38⁺ Th2A cell frequencies following immunotherapy with house dust mite tablet correlates with humoral response. *Clin Exp Allergy* 2021;51:1057-1068.

78. Vieira Braga FA, et al. A cellular census of human lungs identifies novel cell states in health and asthma. *Nat Med* 2019;25:1153-1163.

9. Figure legends

Figure 1. Differentially expressed genes between 127-hi memory cells and CD25-neg memory cells RNA was isolated from sorted 127-hi memory cells and CD25-neg memory cells from either healthy donors (n = 5) or patients with T1D (n = 8) and prepared for bulk RNAseq. Differential gene expression (DGE) of the 127-hi memory cells compared to CD25-neg memory cells was calculated using local false discovery rate (lfdr) also known as the q-value. Genes with less than a lfdr value of 0.3 were considered significant. A) The volcano plots show upregulated (right) and downregulated (left) genes in 127-hi memory compared to CD25-neg memory in Healthy and T1D. Purple arrows point to Th2 associated genes and orange arrows point to Th1-related genes. B) RNAseq data for all 244 healthy and 458 T1D genes that are significantly different between 127-hi and CD25-neg memory cells (from A) were uploaded into the IPA software to identify the top 10 pathways that distinguish 127-hi and CD25-neg memory cell populations in healthy (B, left) and T1D (B, right). C) The top 10 pathways in both healthy and T1D, or healthy only, or T1D only. D) The same RNAseq data from T1D were uploaded into the Cytoscape software and the String Application to identify linked expression of significantly upregulated and downregulated genes using a log ratio equal to or greater than 1. Red symbols represent genes that are upregulated and blue for downregulated genes. Names of genes are indicated on each symbol.

Figure 2. Gene expression associated with 127-hi memory Th2 cell frequency suggests a transcriptional circuitry that is not the same as CD25-neg memory Th2 cells The level of expression of the 458 genes that are significantly differentially expressed in 127-hi compared to CD25-neg memory cells, as determined from the T1D data generated in Figure 1, was correlated with the frequency of 127-hi Th2 and CD25-neg Th2 memory cells in the sorted populations (n = 8). The top 25 strongest positive correlates with 127-hi Th2 memory cell frequency are shown in the left panel in blue and negative correlates in red (A). The correlation between the same genes with CD25-neg Th2 memory cell frequency in the sorted cell populations is shown in the right panel (A). Plots show correlations between 127-hi (B) and CD25-neg (C) Th2 memory cell frequency and Th2-associated genes PRDM1, LRRFIP1, and CCR4, Th17 and regulatory genes ZBTB16 and TIGIT, and Th1-associated genes IL12RB2 and IL6ST. Each symbol represents an individual T1D sample (n = 8). Correlation analysis (r) was performed using Pearson correlations.

Figure 3. The frequency of 127-hi Th2 EM cells positively correlates with LoR PBMC from patients collected within 3 months of diagnosis, were labeled with CD3, CD4, CD25, CD127, CD45RA, CD45RO, CCR7, CXCR5, CXCR3, and CCR4. A. Schematic to show the relationship between the cell subsets analyzed followed by the data showing significance (p) and correlation r (Pearson, Two-tailed) between cell subsets and LoR. Orange and green text shows significant positive correlations between 127-hi memory and Th2 EM and LoR (orange) and between CD25-neg Th2 EM and LoR (green). The frequency of 127-hi Th2 EM (B) and CD25-neg Th2 EM (C), IDAA1c (D) and stimulated C-peptide AUC (E) were determined at baseline and at 3

and 6 and 12 months post-baseline (n = 26). Significant trends were measured using One-way ANOVA with Multiple Comparison. * indicates a p value of 0.05-0.01.

Figure 4. Transcriptome analysis using scRNAseq data identifies cell clusters that are unique to 127-hi memory cells Memory 127-hi and CD25-neg cells were sorted from healthy (n=4) and T1D (n=7) PBMC and prepared for scRNAseq. A-B) A representative example of 127-hi (A) and CD25-neg (B) clusters from an individual with T1D. Each cluster is shown in a different color and each cluster identified by a number. C-D) The number of 127-hi and CD25-neg cells in each cluster in all T1D (C) and Healthy (D) samples. Each symbol represents a separate cluster.

Figure 5. TCR V β V α gene usage in 127-hi Th2 clusters. A) TRBV5-4 and TRAV8-1 expression in 127-hi and CD25-neg cells. B) Expression of GATA3, GATA-AS1, IL9R, PTGDR2, IL4R and CCR7 in 127-hi Th2. Data are from a T1D PBMC sample (T1D #1) and are representative of seven T1D and four Healthy samples.

Figure 6. T cell clonal expansion is evident in Th1, Th2 and Th17 cells Paired TCR sequencing and scRNAseq in 127-hi and CD25-neg cells in a T1D sample (T1D #1). A) Each color on the t-SNE plot represents a single clonotype. Only clonotypes with at least 20 clones are shown. Some clones are spread over several clusters so that a single cluster might have fewer than 20 clones of any one clonotype. B) Th2 (green and purple) and Th1 (blue) cell clusters were identified in 127-hi (i) and CD25-neg (ii) cells. GATA3 (orange) and EOMES (green) expression in 127-hi (iii) and CD25-neg (iv) cells. Clonotypes with greater than 20 clones are shown in black in panels v and vi. C) and D) Magnification of clusters 8 and 11 showing localization of the TCR clonotypes

(C) and expressed Th2-associated genes (D). Arrows point to cells that co-express TCR genes representing clonotypes and Th2-associated genes, GATA3, IL9R and PRGDR2 (C and D). E) Heat map showing the Inverse Simpson's Index in each cluster in all T1D and Healthy samples.

Journal Pre-proof

Table 1A. Th2 clusters identified by upregulation of cell subset-specific markers are predominantly 127-hi cells

Participant ¹	Th ₂ ²	Classical Th1 ³	Non-classical Th1 ⁴	Th1 ₇ ⁵	127-hi in cluster (%) ⁶	CD25-neg in cluster (%) ⁷	Genes used in each cluster ⁸
T1D #1	8				98.0	2.0	GATA3, GATA3-AS1, PTGDR2, IL17RB, IL9R, HPGDS, IL4R

					and CCR7low
T1D #1	11		98.0	2.0	GATA3, GATA3-AS1, PTGDR2, IL17RB, IL9R, HPGDS, IL4R and CCR7low
T1D #2	6		95.7	4.3	GATA3, GATA3-AS1, PTGDR2, IL17RB, IL9R, HPGDS, IL4R and CCR7low
T1D #2	10		94.8	5.2	GATA3, GATA3-AS1, PTGDR2, IL17RB, HPGDS, IL9R, IL4R and CCR7low
T1D #3	10		97.7	2.3	GATA3, GATA3-AS1, PTGDR2, IL17RB, IL9R, HPGDS, IL4R and CCR7low
T1D #1		13	0.6	99.4	GZMA, GZMK, EOMES, IFNG, IFNG-AS1 and CCR7low
T1D #2		2	42.6	57.4	GZMA, GZMK, EOMES, CXCR3 and CCR7low
T1D #2		4	56.7	43.3	GZMA, GZMK, EOMES and CCR7low
T1D #3	8		62.0	38.0	GZMA, GZMK, EOMES, TBX21, IFNG-AS1, IL12RB2, CXCR3 and CCR7+
T1D #5		12	0	100	GZMA, GZMK, EOMES, IFNG-AS1 and CCR7low
T1D #1		3	90.0	10.0	RORC, CCR6, ZBTB16 and CCR7+
T1D #3		3	82.8	17.2	RORC and CCR7+
T1D #3		5	81.7	18.3	RORC, CCR6, ZBTB16 and CCR7+
T1D #5		5	76.8	23.2	RORC and CCR7+
T1D #6		4	82.1	17.9	RORC and CCR7+
Healthy #1	11		0.5	99.5	GZMA, GZMK, EOMES, TBX21, IFNG and CCR7-
Healthy #2		11	58.2	41.8	GZMA, GZMK, EOMES and CCR7-
Healthy #3	10		18.6	81.5	GZMA, GZMK, EOMES, TBX21, IFNG-AS1, IFNG, CXCR3 and CCR7-
Healthy #4		2	45.5	54.5	GZMA, GZMK, EOMES, IFNG-AS1, IL12RB2, CXCR3 and CCR7low
Healthy #3		1	77.8	22.2	RORC, CCR6, ZBTB16 and CCR7+

Table 1B. Th2 and Th1 clusters identified by upregulation of T2 pathway and Th1 pathway genes by IPA

Participant ¹	Th2 ²	Classical Th1 ³	Non-classical Th1 ⁴	127-hi in cluster (%) ⁶	CD25-neg in cluster (%) ⁷	Genes identified using IPA ⁹
T1D #1	(8) ¹⁰			(98.0)	(2.0)	GATA3, PTGDR2, IL17RB, IL4R
T1D #1	(11)			(98.0)	(2.0)	GATA3, PTGDR2, IL17RB, IL4R, CCR3
T1D #2	(6)			(95.7)	(4.3)	GATA3, PTGDR2, IL17RB, IL4R, IL13, CD40,, (down TBX21, IL12RB2)
T1D #2	(10)			(94.8)	(5.2)	GATA3, PTGDR2, IL17RB, CCR3
T1D #3	(10)			(97.7)	(2.3)	GATA3, PTGDR2, IL17RB, IL4R, HLA-DR
T1D #7	1			82.4	17.6	PTGDR2, CCR4, CCR8, BHLHE41, HLA-DR, (down IL12RB2)

T1D #1		4	1.3	98.7	HLA-DP, HLA-DR, ICOS, IL6R, LGALS9
T1D #4		9	11.2	88.8	HLA-DOA, HLA-DQ, HLA-DR, CCR5, CXCR3, LGALS9
T1D #4	11		5.2	94.8	HLA-DP, HLA-DR, ICOS, IL6R, LGALS9
T1D #6		1	5.2	94.8	HLA-DMB, HLA-DQ, TBX21, IL12RB2, CCR5, KLRC1
Healthy #2		10	61.0	39.0	HLA-DMA, HLA-DMB, HLA-DP, HLA-DQ, HLA-DR, CCR5, KLRC1,
Healthy #3		6	3.1	96.9	HLA-DMA, HLA-DR, LGALS9, MAP2K6, TNFSF11
Healthy #3	(10)		(18.6)	(81.4)	HLA-DP, HLA-DQ, HLA-DR, IFNG, IL6R, LGALS9
Healthy #3	11		28.7	71.3	KLRD1, NOTCH2, PIK3CA, PIK3CB, PSEN1
Healthy #4		5	78.3	21.7	HLA-DQ, HLA-DR
Healthy #4		10	4.8	95.2	CD86, HLA-DMA, HLA-DQ, HLA-DR

Table 2. Preferential TCR V β and V α gene usage in Th2, Th1 and Th17 clusters

Participant ¹	Cluster number ²	TCR V β ³	TCR V α ⁴
T1D #1	8	V5-4	V8-1
T1D #1	8	V5-6	
T1D #1	8	V6-6	
T1D #1	8	V7-2	
T1D #1	8	V9	
T1D #1	11	V5-4	V8-1
T1D #1	11	V7-2	V3-2
T1D #3	10	V4-1	V5
T1D #3	10	V7-7	

1. Participant samples with clusters identified as either Th1, or Th2 or Th17. T1D #1 is the sample shown in Figure 4. T1D #2 - #7 and Healthy #1 - #4 are the same as those in Supplemental Data Figure 4 A - J respectively.

2. Clusters identified by DGE of Th2-associated genes (p<0.01)

3. Clusters identified by DGE of Th1-associated genes that include TBX21 (p<0.01)

4. Clusters identified by DGE of Th1-associated genes that include EOMES (p<0.01)

5. Clusters identified by DGE of Th17-associated genes (p<0.01)

6. Frequency of 127-hi cells within a cluster

7. Frequency of CD25-neg cells within a cluster

T1D #3	10	V24-1	
T1D #3	10	V28	
T1D #3	10	V29-1	
T1D #4	9	V6-6	
T1D #4	11	V25-1	V10
T1D #5	12	V13	
T1D #7	1		V10
Healthy #1	11	V14	
Healthy #2	11	V6-4	
Healthy #2	12	V6-4	
Healthy #3	10	V12-5	
Healthy #4	2	V6-8	V13-2
healthy #4	2	V20-1	V34

Table 3. T cell clonal expansion is evident in Th1, Th2 and Th17 127-hi (orange) and CD25-neg

Participant ¹	Cluster number ²	Number of different clonotypes ³	Number of clones per clonotype ⁴	Identified by DGE or IPA ⁵	Cluster cell subset type ⁶
T1D #1	<u>8</u> ⁷	8	220, 147, 26, 25, 15, 11, 8, 2	DGE	Th2
T1D #1	<u>11</u>	8	153, 102, 12, 12, 10, 13, 11, 2	DGE	Th2
T1D #2	<u>6</u>	5	26, 15, 12, 16, 10	DGE	Th2
T1D #2	<u>10</u>	5	10, 9, 14, 7, 8	DGE	Th2
T1D #3	<u>10</u>	5	50, 45, 21, 9, 15	DGE	Th2
T1D #7	1	1	10	IPA	Th2
T1D #1	<u>13</u>	1	21	DGE	non-classical Th1
T1D #2	2	1	15	DGE	non-classical Th1
T1D #2	4	1	11	DGE	non-classical Th1
T1D #4	<u>11</u>	1	25	IPA	classical Th1
T1D #5	5	2	10, 7	DGE	Th17
T1D #6	4	4	6, 10, 9, 3	DGE	Th17
Healthy #1	<u>11</u>	5	131, 86, 73, 45, 22	DGE	classical Th1
Healthy #2	<u>11</u>	2	11, 12	DGE	non-classical Th1
Healthy #3	<u>10</u>	1	42	DGE	classical Th1
Healthy #4	<u>2</u>	5	82, 30, 27, 22, 16	DGE	non-classical Th1
Healthy #4	7	1	14	IPA	non-classical Th1

(green) clusters

Journal Pre-proof

Journal Pre-proof

Graphical Abstract

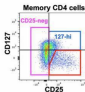
Journal Pre-proof

Highlights

- 127-hi Th2 cells differ transcriptionally from other Th2 cells
- The frequency of 127-hi Th2 cells positively correlates with length of partial remission
- 127-hi cell clonal expansion co-localizes with Th2 cells in paired single cell RNA/TCR sequencing

Journal Pre-proof

In T1D → ↑127-hi cells at diagnosis = ↑ Length of Remission (LoR)



127-hi compared to CD25-neg have a Th2 Bias

Cell Surface markers ↑ CCR4, ↓ CXCR3

Intracellular cytokines ↑ IL-4

Transcription factors ↑ GATA3*

Secreted cytokines ↑ IL-4, ↑ IL-5, ↑ IL-13, ↑ IL-10

Q What confers this Th2 Bias on 127-hi cells?

1

Gene Expression

(Fig. 1, Table 1)

UP	DOWN
IL17RB	GZMA
PTGDR2	GZMK
IL9R	EOMES
GATA3-AS1	IFNG
HPGD5	TBX21
IL4R	IFNG-AS1
	IL12RB2
	HLA-DR

2

Molecular Pathways

(Fig. 1, Table 1B)

Th2	↑
Th1 & Th2 activation	↑
Th cell differentiation	↑
IL-4 signaling	↑

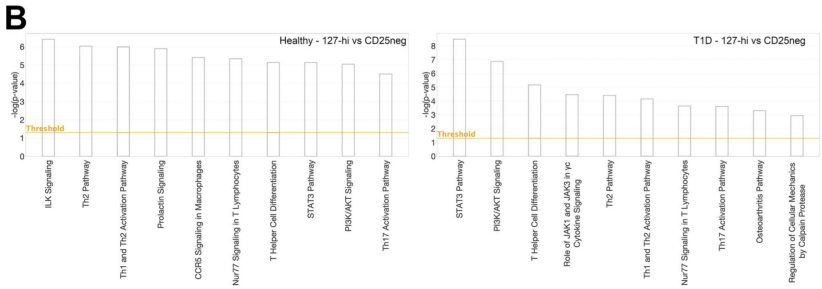
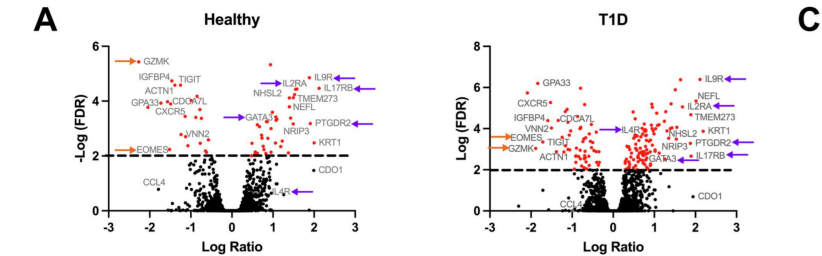
3

Clonal Expansion

(Fig. 7)

Condition	Cell subset	Th2 clones	Th1 clones
T1D	127-hi	Yes	No
T1D	CD25-neg	No	Yes
Healthy	127-hi	No	Yes
Healthy	CD25-neg	No	Yes

Graphics Abstract



C

Healthy and T1D	T1D only
Th2 pathway	JAK1/JAK3 in γ c Cytokine Signaling
Th1 and Th2 activation pathway	Osteoarthritis Pathway
T helper cell differentiation	Regulation of Calpain Protease
Th17 activation pathway	Healthy only
Nur77 signaling in T lymphocytes	ILK Signaling
STAT3 pathway	Prolactin Signaling
PI3K/AKT signaling	CCR5 Signaling in macrophages

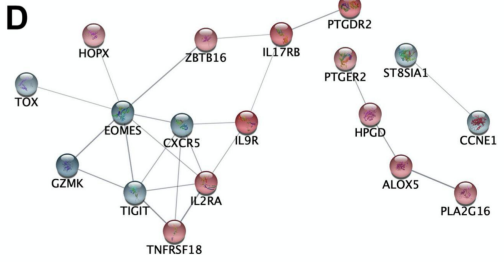


Figure 1

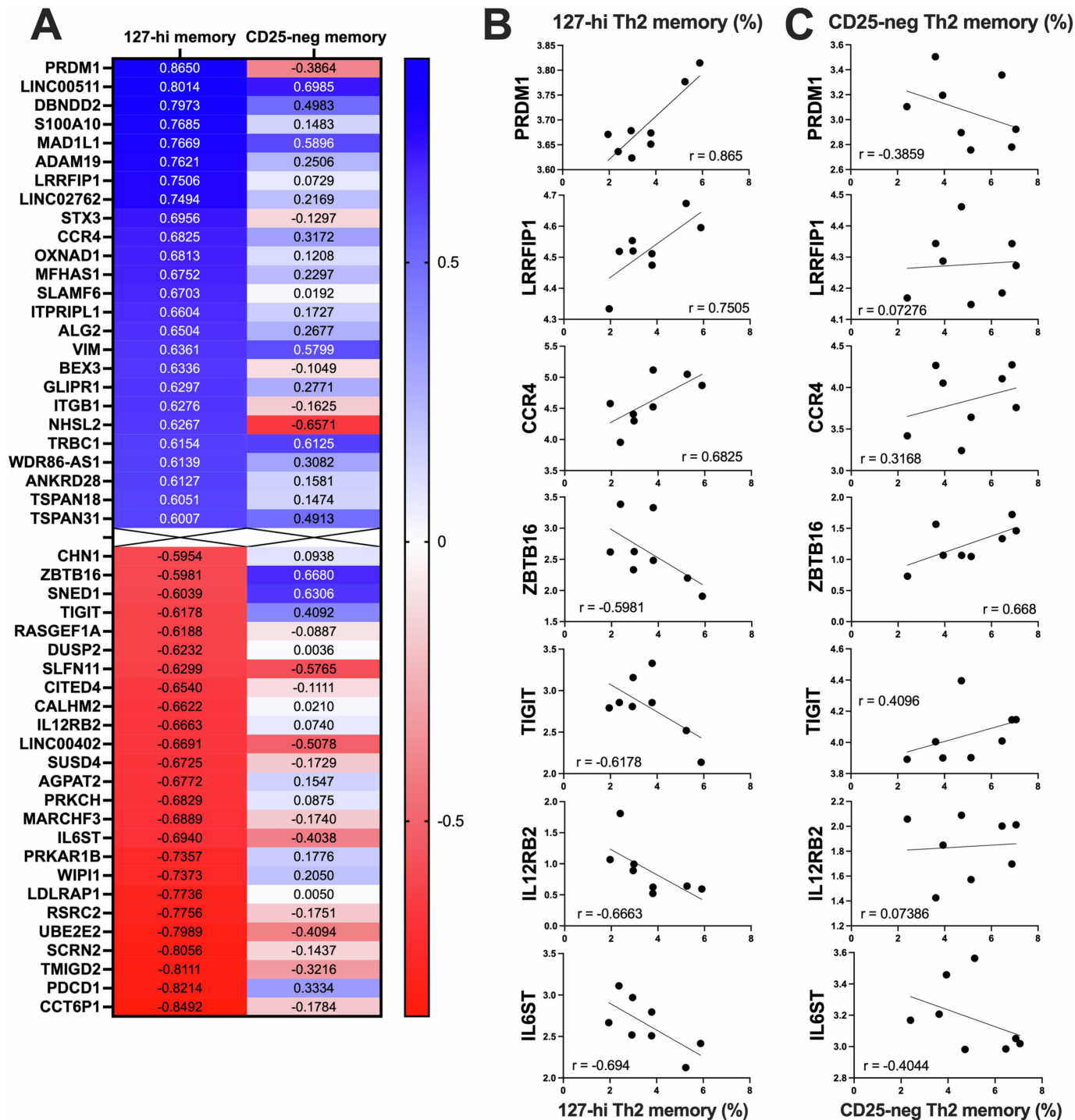
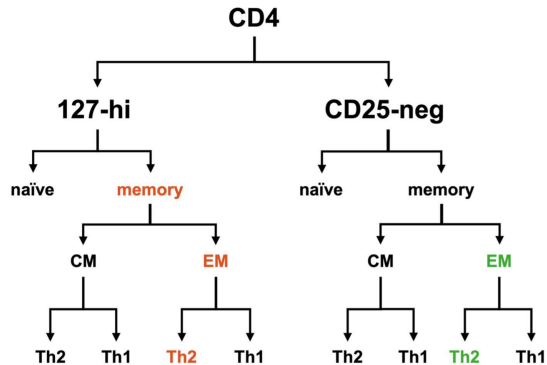


Figure 2

A

Correlation between cell subset frequency and LoR

Cell subset	127-hi (p value)	CD25-neg (p value)	127-hi (correlation r)	CD25-neg (correlation r)
memory	0.03	0.40	0.42	0.17
Th2 CM	0.09	0.12	0.35	0.32
Th1 CM	0.71	0.72	0.08	-0.07
Th2 EM	0.003	0.03	0.55	0.42
Th1 EM	0.25	0.19	0.24	0.27

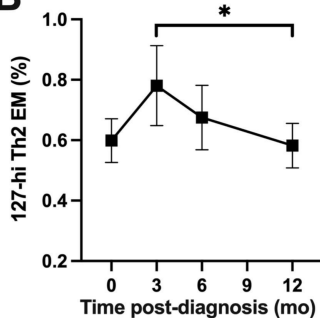
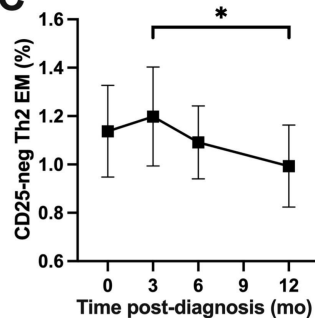
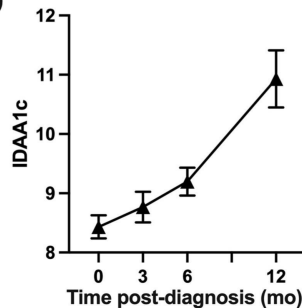
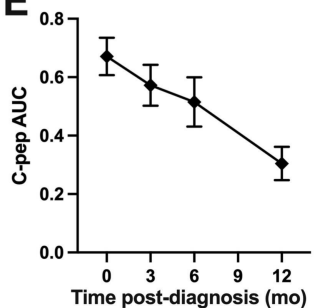
B**C****D****E**

Figure 3

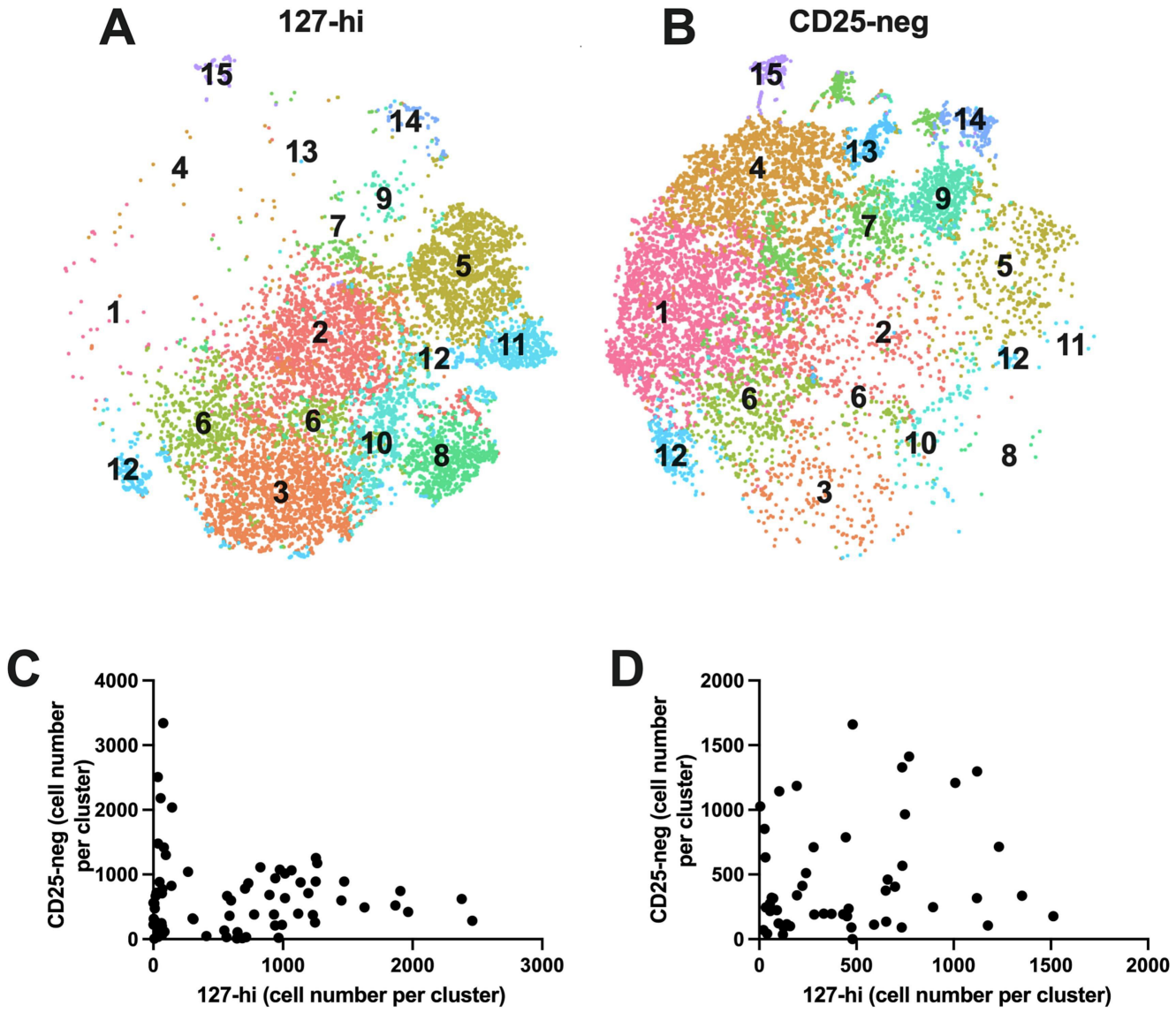
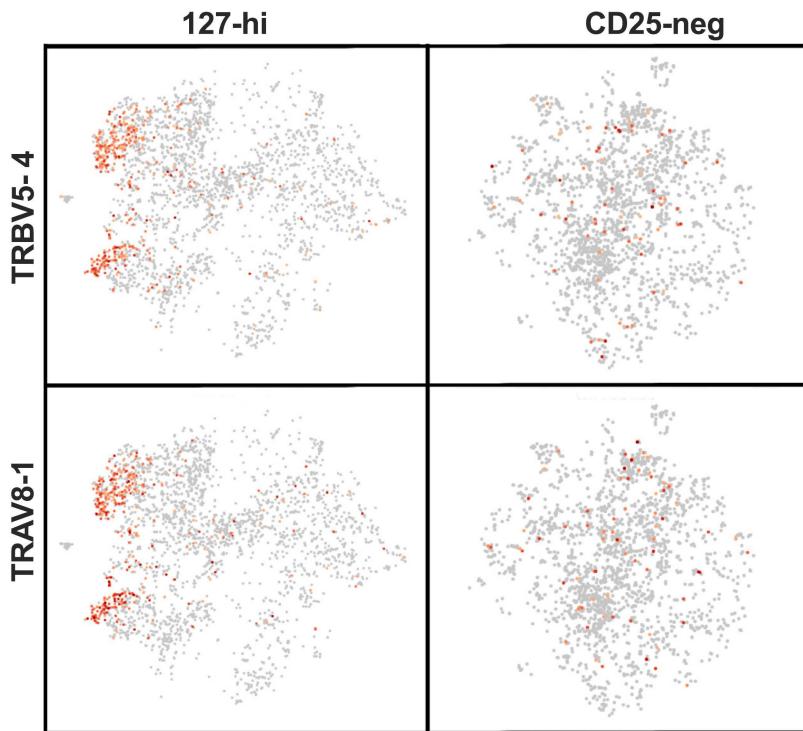


Figure 4

A**B**

127-hi

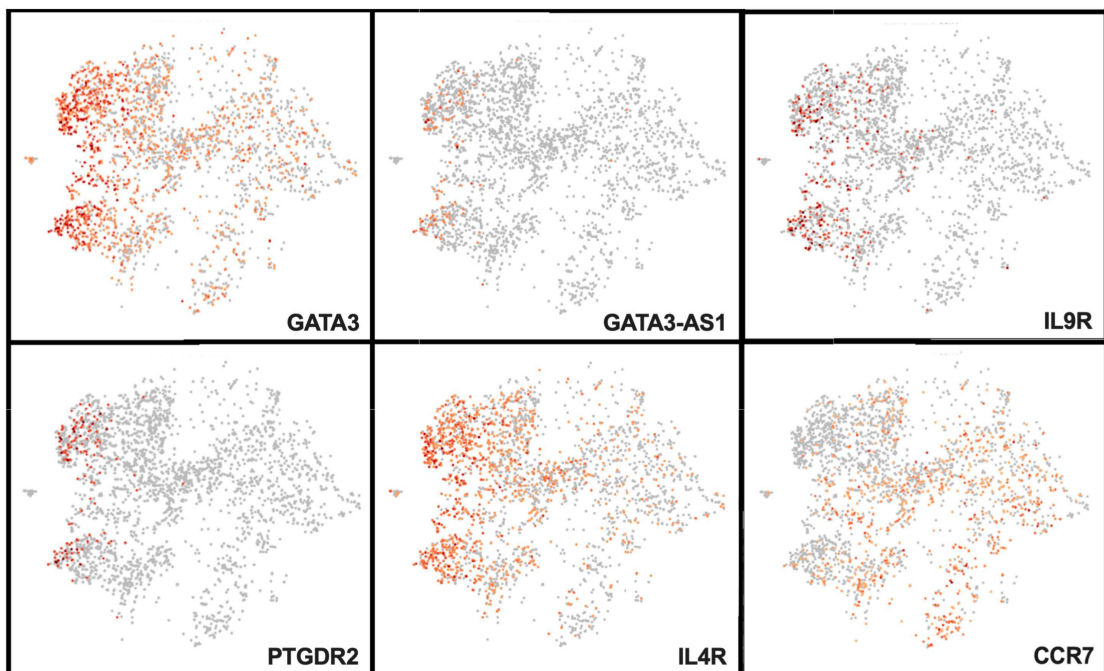


Figure 5

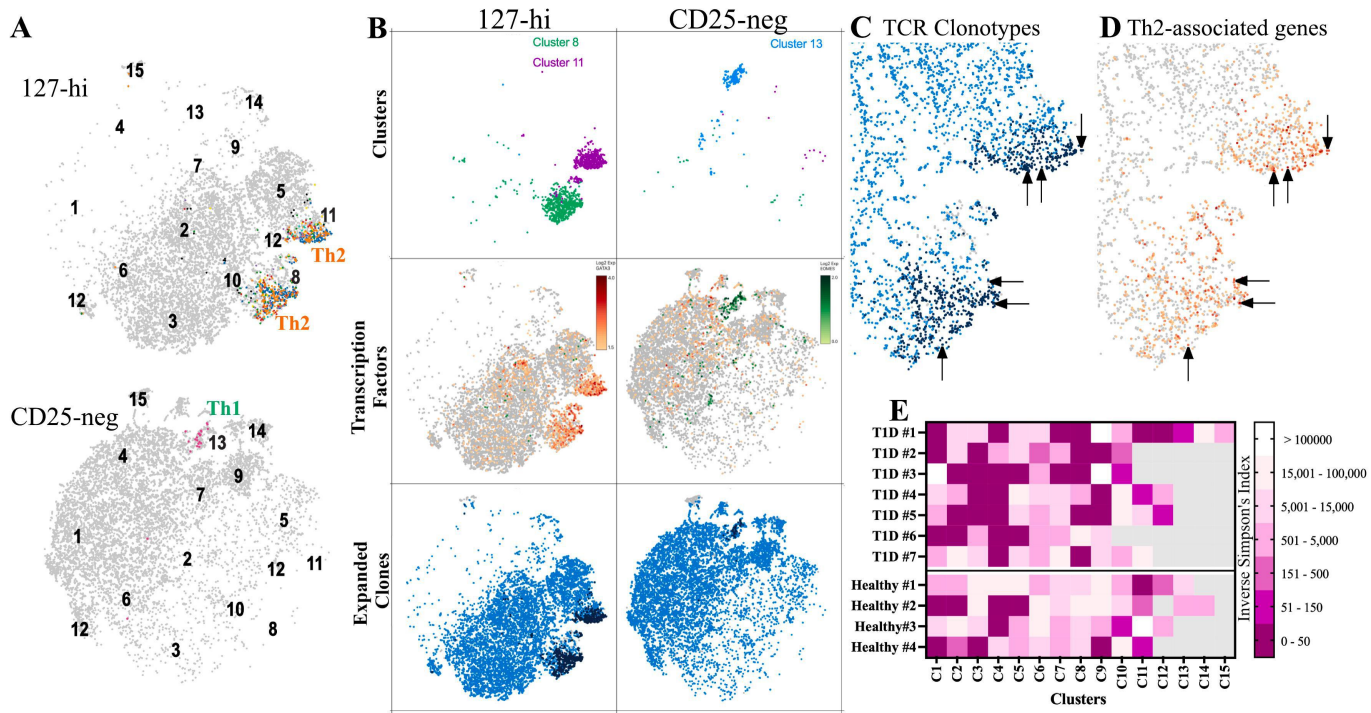


Figure 6